A Comprehensive Overview of Engineering Sciences and the Trends of Modern Engineering

A Comprehensive Overview of Engineering Sciences and the Trends of Modern Engineering

Edited by

Francisco Bulnes

Cambridge
Scholars
Publishing

A Comprehensive Overview of Engineering Sciences and the Trends of Modern Engineering

Edited by Francisco Bulnes

This book first published 2024

Cambridge Scholars Publishing

Lady Stephenson Library, Newcastle upon Tyne, NE6 2PA, UK

British Library Cataloguing in Publication Data
A catalogue record for this book is available from the British Library

ISBN (10): 1-5275-5618-2
ISBN (13): 978-1-5275-5618-8

CONTENTS

ACKNOWLEDGEMENTS

The academic editor, Dr Francisco Bulnes, is grateful to all the organizing committees who helped in the administrative procedures, asking for and providing the facilities, materials and financing sources for the First Conference in Engineering Sciences (SCIENSETECH) in TESCHA (Tecnológico de Estudios Superiores de Chalco). Likewise, in order of hierarchy, Lic. Guillermo Gustavo Falcón-Torres, TESCHA General Director, Accounter Sandra Estrella García-Castro, TESCHA Financing and Administration Director, Master of Science Roberto Leguízamo-Jiménez, TESCHA Academic Director, Accounter María del Rosario Leyte-Zárate, TESCHA Research and Postgraduate Subdirector. The five heads of Engineering Career Divisions, Eng. Rene Rivera-Roldán, Electronics Engineering Programme, Eng. Máximo Livera-Leónides, Electromechanical Engineering Programme, M. D. IT. Marino Zuñiga-Domínguez, Informatics Engineering Programme, MsC. Blanca Inés Valencia-Vazquez, Computational Systems Engineering Programme, M. IR. Vianca Lisseth Pérez-Cruz, Industrial Engineering Programme, and Eng. Francisco López.

Also, my acknowledgements to the following organizing committees, who helped me with the logistics and operation of this important conference:

My Executive and Personal Committee

Eng. Rocío Cayetano-Meléndez, Editorial
MsC. Martha Guadalupe Morales-Huerta, Logistics
MsC. Mercedes Ramírez-Valdez, Logistics

Academic Committee

MsC. Jorge Tello-Cruz
Dr. Claudio López-García
Dr. Luis Manuel Valverde-Cedillo
Dr. Gloria Tenorio-Sepúlveda

Material Resources and Infrastructure Committee
Eng. Lorenzo Ávila-García
MsC. Guadalupe Nayeli Villanueva-Valdivia
Lic. Cristóbal Estrada-Acosta

Logistics Committee
M. I. David Cote-Sánchez
Eng. Miriam Denisce Sánchez-Sánchez
M. RI. Eulalia Ventura-Mójica
Dr. Jarumi Aguilar
Eng. Rebeca Reyes-de la Rosa
MsC. Raul Romero-Castro
MsC. Claudia Guzmán-Barrera

PREFACE

The systematic and modern study of science to establish the trends of engineering for the future development of technology and vanguard technologies are transducers, material sciences, MEMs, plasmonics, quantum computing and communication, advanced programming, artificial intelligence, advanced manufacturing, nanotechnology, semiconductors and superconductors, microcircuits, optics-electronics, advanced informatics devices, etcetera. All this conforms to the development of modern engineering.

SCIENCETECH (1st Conference on Engineering Sciences) will function as a disseminator of knowledge through presentations of high levels of research, dissemination, perspective and development of technology in order to encourage a taste for engineering and science, something fundamental for the development of the region, the state of Mexico, the country and humanity. Engineering creates a country's wealth from genius based on mathematics and physics and not from being an administrator for other people's wealth.

Dr Francisco Bulnes,
Head of Research Department in Mathematics and Engineering,
TESCHA, IINAMEI Director

Excmo. Prof. Dr. Dr h. c. Francisco Bulnes-Aguirre, First Adviser and Worldwide Director of International Conferences

CHAPTER 1

ADVANCED MATHEMATICAL TECHNIQUES FOR THERMAL DESIGN OF POWER TRANSFORMERS

ALEJANDRO ROBERTO TELLO-CAMPOS

1.1 Introduction

Power transformers are key elements in the electrical industry. These devices involve converting electrical power from a high voltage to a low voltage level. In this way, these devices can transmit power from a generating power station to power consumption centres located in industrial industries and domestic centres such as houses or commercial centres. The efficiency of power transformers is quite high, but at present, researchers have been investigating ways to improve the heat dissipation derived from the circulating windings in the electrical conductors of these apparatuses. In the studies presented, the temperatures of windings and the oil dynamics of a power transformer are studied. In the first part of this chapter, a presentation of advanced mathematical techniques is depicted. Then, CFD techniques are used in 3D and 2D models varying oil velocities to obtain contours of oil velocities and temperatures, indicating how the heat dissipation occurs in the windings and core.

Different techniques have been developed to study the heat dissipation in power transformers. Among them, advanced mathematical techniques have employed Hankel and Fourier transforms to solve the heat conduction equation for a cylindrical winding. Other researchers have used CFD to solve the continuity, momentum, and energy equations encountered in the natural and forced convection of cooling oil used for the cooling of the windings of power transformers. 2D and 3D models have helped researchers

study the dynamics of oil flow, which determines the optimum cooling of windings and the location of the maximum temperature, which could deteriorate the properties of oil and reduce the life of the electrical transformers.

Some researchers using reduced 2D models have reported the formation of oil streaks at the outlet of horizontal cooling channels due to the intense mixing of hot oil from the vertical cooling channels and cold oil from the horizontal cooling channels. Also, a swirling flow of oil has been observed when oil encounters adverse pressure gradients in the cooling channels in the same simplified 2D models.

Little work has been done regarding the use of 3D models because of the complexity of the calculations performed by the computer, therefore increasing the computation time. This chapter presents the heat diffusion equation of a typical winding. Then, whole 2D and 3D models have been used to study the dynamics of oil when conditions of forced cooling oil have been set in the power transformer. Three oil velocities were used with one and two inlet geometries.

1.2 Advanced Mathematical Techniques

The construction of a power transformer consists of a tank normally made out of carbon steel, which, in the case of a 3-phase device, contains a set of three windings, each of them composed of high and low-voltage coils forming a high-voltage circuit normally connected to a power generating station and a low voltage circuit connected to a domestic use or industrial load. See Figure 1.

Figure 1

The windings are constructed with copper or aluminium electrical conductors, which allow the circulation of currents. In Figure 2, a typical winding construction is depicted with the supporting structures and oil cooling channels.

Figure 2

In order to evaluate the heat dissipation caused by the Joule effect due to the electrical currents circulating in the windings, geometry composed of a winding is considered for the analysis. The governing equation for this case is the heat conduction equation, which is presented here:

$$\frac{\partial^2 T}{\partial r^2} + 1/r\frac{\partial T}{\partial r} + \frac{\partial^2 T}{\partial z^2} + \frac{\partial^2 T}{\partial \theta^2} + G/K = 0 \quad (1)$$

As the temperature is varying only with the coordinates r and z, the above equation is simplified to the following form:

$$\frac{\partial^2 T}{\partial r^2} + \frac{\partial^2 T}{\partial z^2} + G/K = 0 \qquad (2)$$

The boundary conditions are as follows:

on the inner surface of the cylinder:

$$-k_1 * \frac{\partial T}{\partial r} + h_1 * T = f_1(r) \qquad (3)$$

on the outer surface of the cylinder:

$$-k_2 * \frac{\partial T}{\partial r} + h_2 * T = f_2(r) \qquad (4)$$

on the bottom surface of the cylinder:

$$-k_3 * \frac{\partial T}{\partial r} + h_3 * T = f_3(r) \quad (5)$$

on the top surface of the cylinder:

$$-k_4 * \frac{\partial T}{\partial r} + h_4 * T = f_4(r) \quad (6)$$

$$f_1(r) = h_1\,(T_b) \qquad (7)$$

$$f_2(r) = h_2\,(T_b) \qquad (8)$$

$$f_3(r) = h_3\,(T_b) \qquad (9)$$

$$f_4(z) = T_4\,(T_t) \qquad (10)$$

Taking the Hankel transform of the first term of equation (2):

$$[\int_a^b (\frac{\partial^2 T}{\partial r^2} + 1/r\frac{\partial T}{\partial r}) K_0(\beta_{n\,,r}) r dr] = r\frac{\partial T}{\partial_r} K_0(\beta_{n\,,}r)\Big|_a^b -$$

$$Tr\beta_n K_0'(\beta_{n\,,}r)\Big|_a^b + [\int_a^b T\ \frac{d}{dr}\beta_{n\,,} r K_0'(\beta_{n\,,}r) dr] \qquad (11)$$

Evaluating the last term of equation (11):

$$\frac{d}{dx}\beta_n, rK_0'(\beta_n, r)dr = -\frac{d}{dr}\beta_n r K_1(\beta_n, r) =$$

$$-\frac{d\beta_{n,r}}{dr}[\frac{d}{d(\beta_n, r}(\beta_n, r)K_1(\beta_n, r)] = -\beta_n^2 r K_0(\beta_n, r) \quad (12)$$

then:

$$[\int_a^b T(r,z)\frac{d}{dr}\beta_n, rK_0'(\beta_n,r)dr]=[\int_a^b T(r,z)(-\beta_n^2 rK_0(\beta_n,r))dr] = -\beta_n^2\,\bar{\bar{T}}(\beta_n,r). \quad (13)$$

Considering the boundary conditions of equations (3) to (6):

$$-k_1\beta_n\frac{dR_0}{\beta_n r}+h_1R_0=0;\;\; k_2\beta_n\frac{dR_0}{\beta_n r}+h_2R_0=0 \quad (14)$$

where:

$$R_0'=(h_1/\beta_n k_1)R_0 \quad (15)$$
$$R_0'=(h_2/\beta_n k_2)R_0 \quad (16)$$

and:

$$K_0'=(h_1/\beta_n k_1)K_0 \quad (17)$$
$$K_0'=(h_2/\beta_n k_2)K_0 \quad (18)$$

then:

$$K_0(\beta_n,r)=R_0(\beta_n,r)\sqrt{N}=(2/b)1/h_2+k_2+1 \quad (19)$$

Expanding the terms of equation (11):

$$\frac{\partial T}{\partial r}rK_0(\beta_n,r)+Tr(h_2/k_2)K_0(\beta_n,r)_{r=b}-\frac{\partial T}{\partial r}rk_0(\beta_n,r)+Tr(h_1/k_1)K_0(\beta_n,r)_{r=a} \quad (20)$$

and considering:

$$\frac{\partial T}{\partial r_{r=a}}=(h_1/k_1)T-(f_1(z)/k_1)_{r=a} \quad (21)$$

$$\frac{\partial T}{\partial r_r}=b=(h_2/k_2)T-(f_2(z)/k_2)_{r=b} \quad (22)$$

from equation (11):

$$[\int_a^b (\frac{\partial^2}{\partial r^2} \quad +1/ \quad r\frac{\partial T}{\partial r}) K_0(\beta_n, r) r dr] = (f_2/k_2)(rK_0(\beta_n, r)_{r=b} + (f_1/k_1)$$
$$(rK_0(\beta_n, r)_{r=a} - \beta^2 T \qquad (23)$$

And for the second term of equation (2):

$$[\int_a^b (\frac{\partial^2 T}{\partial z^2}) + G/k r K_0(\beta_n, r) dr] = (\frac{\partial^2}{\partial^2 z})[\int_a^b rTK_0(\beta_n, r) dr] + [\int_a^b (G_0 +$$
$$g_0/k)\, rK_0 dr] = \frac{d^2\bar{T}}{dz^2} + \overline{G_0}\ /\text{k+}(g_0\rho\bar{T}\ /k)(24)$$

the solution of equation (2) considering (23) and (24):

$$-\beta_n^2 \overline{T}(\beta_n, z) + f_2(z)/k_2 rK_0(\beta_n, r)_{r=b} + f_1/k_1 rK_0(\beta_n|, r)_{r=a} +$$
$$\frac{d^2\bar{T}}{dz^2} + \overline{G_0}/k + g_0/k = 0 \qquad (25)$$

Applying the finite Fourier transform to the second term of equation (25):

$$[\int_a^b \frac{d^2 T}{dz^2} M(\alpha_m, z) dz] = \frac{d\bar{T}}{dz} M(\alpha_m, z)_{z=0}^{\iota} - \bar{T}\ \alpha_m M'(\alpha_m, z)_{z=0}^{\iota} +$$
$$[\int_a^b \alpha_m^2\, \overline{T}\, M''(\alpha_m, z) dz] \quad (26)$$

expanding the first two terms:

$$[\frac{d\bar{T}}{dz} - \bar{T}\alpha_m M'(\alpha_m, z)]_{z=\iota} - [\frac{d\bar{T}}{dz} - \bar{T}\ \alpha_m M'(\alpha_m, z)]_{z=0} (27)$$

considering the boundary conditions:

$$M'(\alpha_m, z)_{z=0} = (h_3/k_3) M(\alpha_m, z)_{z=0} \quad (28)$$

$$M'(\alpha_m, z)_{z=1} = (h_4/k_4) M(\alpha_m, z)_{z=\iota} \quad (29)$$

and:

$$\frac{d\bar{T}}{dZ_{z=0}} = [(h_3/k_3)\bar{T} - \bar{f_3}\ (\beta_n/k_3)]_{z=0} \qquad (30)$$

$$\frac{d\bar{T}}{dZ_{z=0}} = [(h_4/k_4)\bar{T} - \bar{f}_4(\beta_n/k_4]_{z=\iota} \qquad (31)$$

substituting:

$$\frac{d\bar{T}}{dz}M(\alpha_m, z)_{z=0}^{\iota} = \bar{f}_4(\beta_n)[M(\alpha_m, z]_{z=\iota} + \bar{f}_3(\beta_n)[M(\alpha_m, z]_{z=0} \quad (32)$$

the third term is

$$\int_a^b \alpha_m^2 \bar{T}(\beta_n, z)M''(\alpha_m, z)dz = -\alpha_m^2 \int_a^b \bar{T}\,(\beta_n, z)\, M(\alpha_m, z)dz = -\alpha_m^2 \bar{T}\,(\beta_n, \alpha_m) \quad (33)$$

$$\int_a^b \frac{d^2\bar{T}}{dz^2}M(\alpha_m, z)dz = \frac{\bar{f}_4\,(\beta_n)}{k_4}M(\alpha_m, z)_{z=\iota}\frac{\bar{f}_3\,(\beta_n)}{k_3}M(\alpha_m, z)_{z=0} - \alpha_m^2 T(\beta_n, \alpha_m) \quad (34)$$

then:

$$T(r, z) = \sum_{n=1}^{\infty}\sum_{m=1}^{\infty}\bar{T}\,(n, \alpha_m)K_0(\beta_n, r)M(\alpha_m, z) \quad (35)$$

where:

$$K_0(\beta_n, r) = \frac{R_0(\beta_n, r)}{\sqrt{N}} \qquad (36)$$

$$N = \int_a^b rR_0^2(\beta_n, r)\, dr = [\frac{r^2}{2}R_0'^2(\beta_n, r)]|_a^b \quad (37)$$

$$R_0'^2 = \frac{dR_0(\beta_n, r)}{d(\beta_n, r)} \qquad (38)$$

$$N = \frac{b^2}{2}(\frac{h_2^2}{\beta_n^2 k^2} + 1)R_0^2(\beta_n, b) - \frac{a^2}{2}(\frac{h_1^2}{\beta_n^2 k^1} + 1)R_0^2(\beta_n, a) \quad (39)$$

$$M(\alpha_m, z) = \frac{Z(\alpha_m, z)}{\sqrt{N}} \qquad (40)$$

$$N = \left[\frac{\alpha_m^2 + \frac{h_3^2}{k_3^2}}{\alpha_m^2}\left(1 + \frac{\frac{h_4}{k_4}}{\alpha_m^2 + \frac{h_4^2}{k_4^2}}\right) + \frac{\frac{h_3}{k_3}}{\alpha_m^2}\right] \qquad (41)$$

1.3 CFD techniques

The 3D power transformer model consists of three cylindrical windings set in a simplified core. The windings are solid copper cylinders, dissipating heat to the surrounding cooling oil. Although the core is usually composed of laminated sheets of iron, which help maintain the coils' position within the tank and provide a path for the magnetization current, simplifying a solid rectangular iron core dissipating heat to the surrounding oil is also considered. Figures 3a and 3b show the geometries considered for the power transformer's one and two oil inlets.

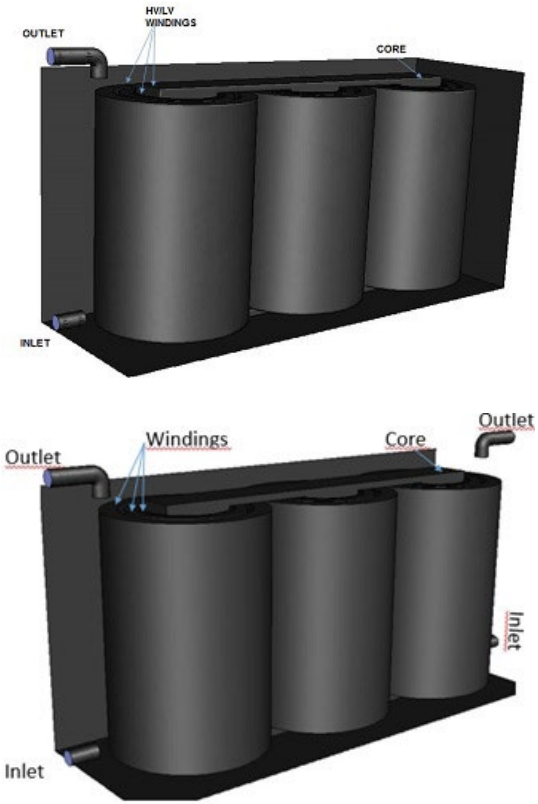

Figures 3a and b

Note. The model was simulated using the continuity, momentum and energy equations as follows:

$$divV = 0$$

In the X-direction

$$u\frac{\partial u}{\partial x}+v\frac{\partial u}{\partial y}+w\frac{\partial u}{\partial z}= -1/\rho\frac{\partial p}{\partial x}+v(\frac{\partial^2 u}{\partial x^2}+\frac{\partial^2 u}{\partial y^2}+\frac{\partial^2 u}{\partial z^2})$$

In the Y-direction

$$u\frac{\partial v}{\partial x}+v\frac{\partial v}{\partial y}+w\frac{\partial v}{\partial z}= -1/\rho\frac{\partial p}{\partial y}+v(\frac{\partial^2 v}{\partial x^2}+\frac{\partial^2 v}{\partial y^2}+\frac{\partial^2 v}{\partial z^2}) \quad (3)$$

In the Z-direction

$$u\frac{\partial w}{\partial x}+v\frac{\partial w}{\partial y}+w\frac{\partial w}{\partial z}= -1/\rho\frac{\partial p}{\partial z}+v(\frac{\partial^2 w}{\partial x^2}+\frac{\partial^2 w}{\partial y^2}+\frac{\partial^2 w}{\partial z^2})$$

Energy equation

$$u\frac{\partial T}{\partial x}+v\frac{\partial T}{\partial y}+w\frac{\partial T}{\partial z}=\frac{k}{\rho\, Cp}(\frac{\partial^2 T}{\partial x^2}+\frac{\partial^2 T}{\partial y^2}+\frac{\partial^2 T}{\partial z^2})+\mathrm{Se}$$

The above equations are considered along with the flotation term, which represents the variation of fluid density with gravity. Also, the properties of the fluid are dependent on temperature as follows:

$$\rho(T)=1098.72-0.72T$$
$$k(T)=0.1509-7.101E-05T$$
$$c_p(T)=807.163+3.58T$$
$$\mu'(T)=0.08467-0.0004T+5E-7T^2$$
$$T \text{ in } K$$

The equations are discretized and solved using an embedded algorithm in the ANSYS Fluent FEM code. The boundary conditions are:

a) Tank walls, windings, and the core are considered non-slip boundaries.
b) The outlet is considered a zero-pressure condition.
c) Inlet oil velocities of 0.002 m/s, 0.05 m/s, and 0.1 m/s.
d) An inlet oil temperature of 298 K.
e) Fixed heat generation of 7.87 W/m2 for the core, 5.18 W/m2 for the LV winding, 1.94 W/m2 for the HV winding, and 2.94 W/m2 for the regulating winding.

1.4 Results and Discussion

Contours of temperature were obtained for the two power transformer geometries for the case of 0.002 m/s. These are shown in Figures 4 and 5.

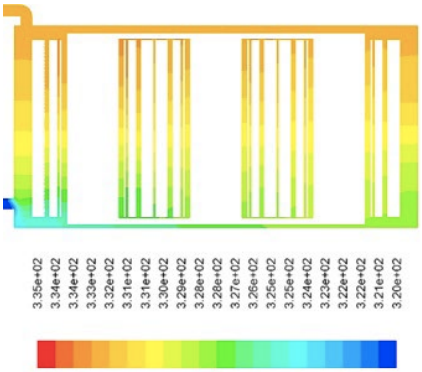

Figure 4

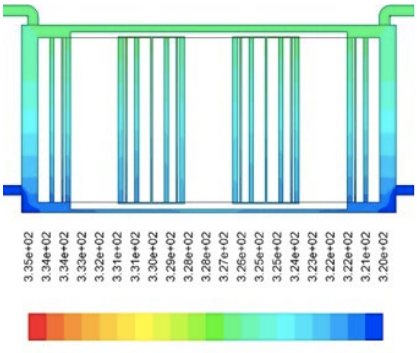

Figure 5

From Figures 4 and 5, the oil temperature is clearly high for the one inlet geometry. This can be thought of as heat dissipation being more efficient when using two-inlet geometry. More cold oil is reaching the inner windings. The maximum oil temperature at the top of the windings was 331 K for the one inlet geometry and 327 K for the two inlet geometry.

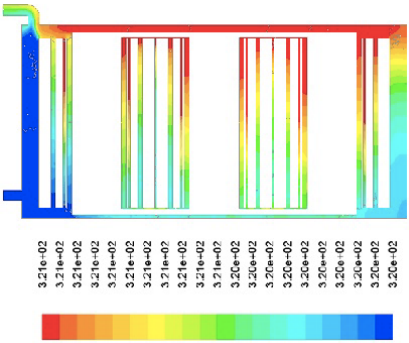

Figure 6

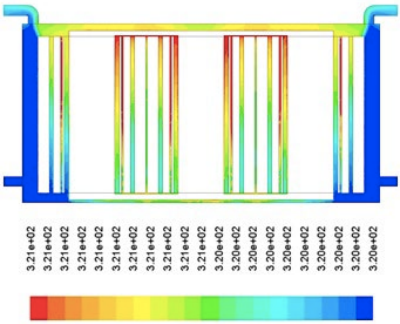

Figure 7

The same trend observed previously for the case of 0.002 m/s is depicted in Figures 4 and 5 for the 0.5 m/s case. The one inlet geometry shows an increase in oil temperature at the top of the windings while the two inlet geometry shows less increase in oil temperature and, therefore, a more efficient cooling of the power transformer. The maximum value of oil temperature was 321 K at the top of the windings for the one inlet geometry, while it was 321 K at the outer surface of the LV windings.

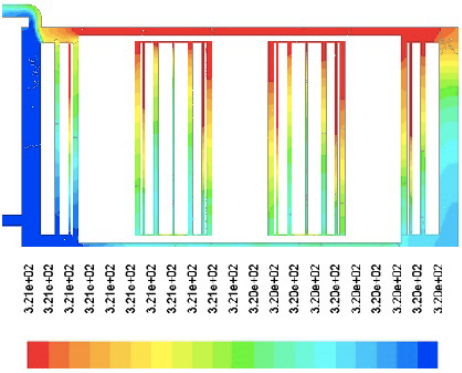

Figure 7

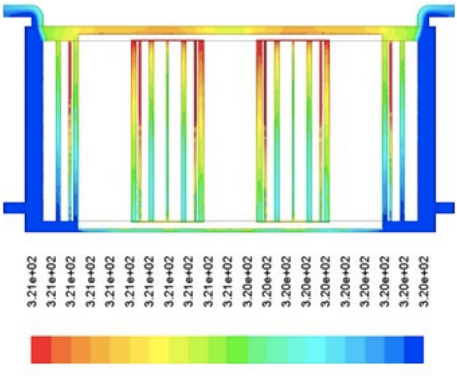

Figure 8

A little improvement in cooling efficiency is shown in Figures 7 and 8. The maximum oil temperature is 321 K for the one inlet and two inlet geometries. The difference is the location of the maximum oil temperature at the top of the windings for the one inlet geometry and at the outer surface of the LV windings.

Figures 8 and 9 show the oil velocity vector graphics for the one and two inlet geometries for the 0.002 m/s case.

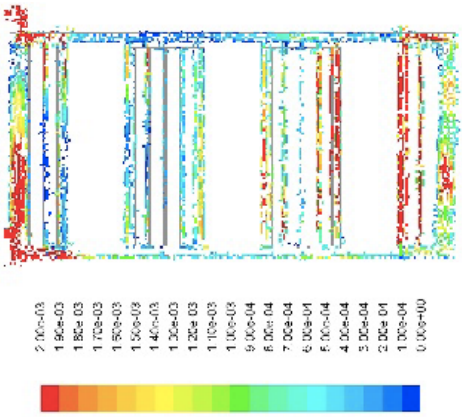

Figure 9

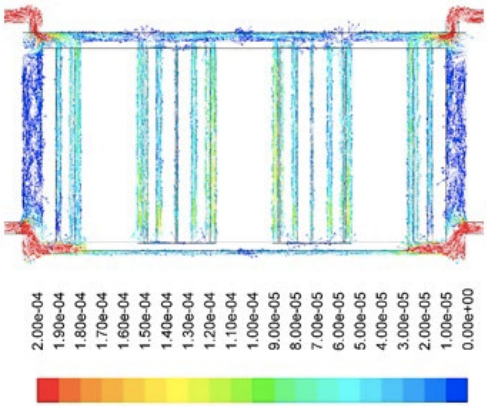

Figure 10

Oil is circulating through the less hydraulic resistance path. In the case of the one-inlet geometry, oil reaches the outlet at a higher velocity through the side of the winding close to the inlet. Due to a kind of siphon effect, some oil reaches the furthest winding from the inlet with high velocity. In the case of two inlet geometry, oil is more evenly distributed through the windings at relatively high velocities.

The so-called oil streaks have not been observed because the geometries presented in the analysis do not include a disc geometry for the windings.

In the case of 0.05 m/s, oil velocities vectors are depicted in Figures 11 and 12.

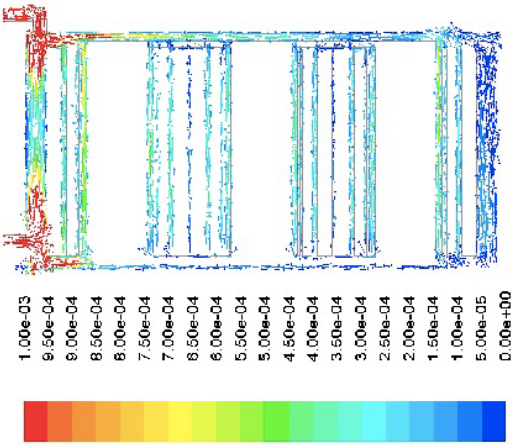

Figure 11

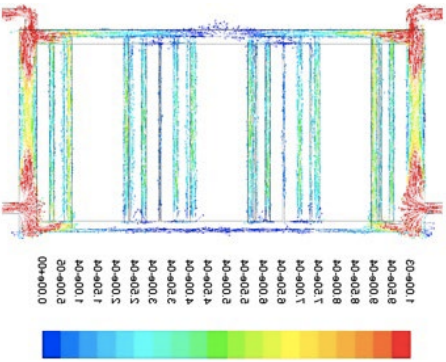

Figure 12

Figures 13 and 14 show a more distinct feature: some stagnant flow is depicted at the vertical oil cooling channels of the windings for the one inlet geometry, being more centralized for the two inlet geometry. The zone of maximum oil velocities occurs at the oil inlet and outlet due to the less hydraulic resistance effect previously mentioned.

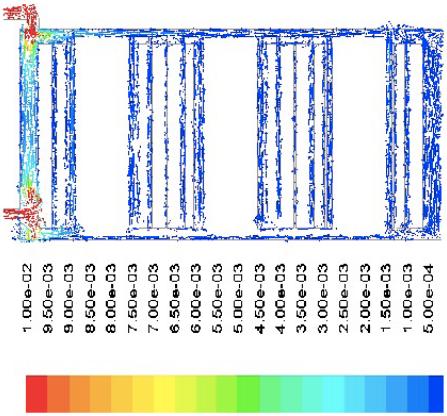

Figure 13

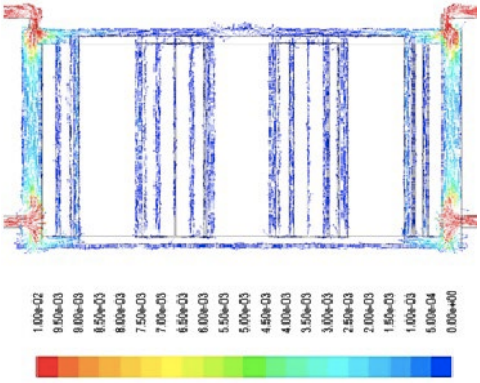

Figure 14

Oil flows at higher velocities from the inlets to the outlets following the less hydraulic resistance path. Also, high oil velocities are encountered in the vertical oil cooling channels located at the windings.

The 2D model considered was a copper disk winding configuration along with the solid iron core. The same equations of continuity, momentum and energy were considered, and the geometry uses only one oil inlet and outlet.

The contours of oil velocity and temperature are shown in Figures 15 and 16.

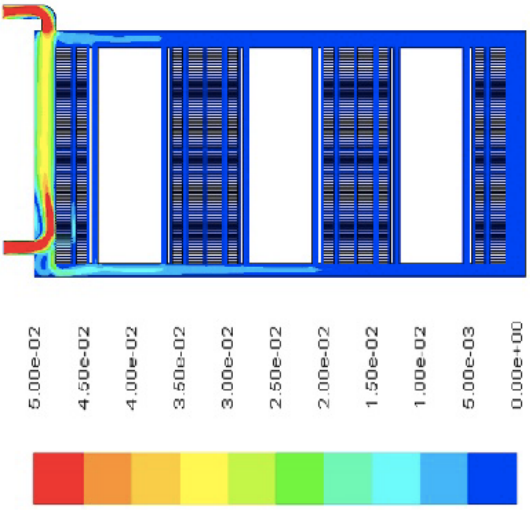

Figure 15

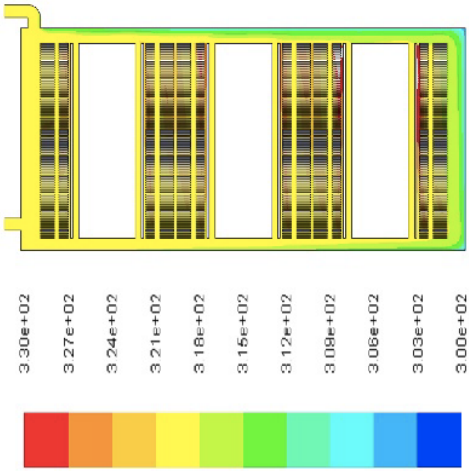

Figure 16

As previously established in the 3D model using copper solid windings, the 2D model using copper disks Figure 14 shows the same pattern concerning the oil movement within the power transformer tank.